

# Pharmacological properties of homomeric and heteromeric GluR1<sub>o</sub> and GluR3<sub>o</sub> receptors

Brian S. Nielsen, Tue G. Banke, Arne Schousboe, Darryl S. Pickering \*

PharmaBiotec Research Center, Department of Pharmacology, The Royal Danish School of Pharmacy, 2 Universitetsparken, DK-2100 Copenhagen, Denmark

Received 29 June 1998; accepted 11 September 1998

## Abstract

Homomeric and heteromeric  $\alpha$ -amino-3-hydroxy-5-methyl-4-isoxazolepropionate (AMPA) receptor subunits GluR1<sub>o</sub> and GluR3<sub>o</sub> were expressed in *Spodoptera frugiperda* (Sf9) insect cells. Membranes containing the recombinant receptors showed a doublet of bands of the expected size (99–109 kDa) after western immunoblotting which was shifted to a single band upon deglycosylation. In (*R,S*)-[<sup>3</sup>H]AMPA binding experiments, high expression was seen ( $B_{\max} = 0.8\text{--}3.8$  pmol/mg protein) along with high affinity binding to a single site ( $K_d$ , nM  $\pm$  S.D.): GluR1<sub>o</sub>,  $32.5 \pm 2.7$ ; GluR3<sub>o</sub>,  $23.7 \pm 2.4$ ; GluR1<sub>o</sub> + GluR3<sub>o</sub>,  $18.1 \pm 2.9$ . The pharmacological profiles of these receptors resembled that of native rat brain AMPA receptors: AMPA analogues > L-glutamate > quinoxaline-2,3-diones > kainate. In the *Xenopus* oocyte expression system we had previously shown that the agonist (*R,S*)-2-amino-3-(3-carboxy-5-methyl-4-isoxazolyl)propionate (ACPA) exhibited an 11-fold selectivity for GluR3<sub>o</sub> vs. GluR1<sub>o</sub>. In this study, it was found that ACPA has ~3-fold higher affinity at homomeric GluR3<sub>o</sub> and heteromeric receptors than at homomeric GluR1<sub>o</sub>, suggesting that its efficacy and/or desensitisation properties are different at GluR1<sub>o</sub> vs. GluR3<sub>o</sub>. © 1998 Elsevier Science B.V. All rights reserved.

**Keywords:** AMPA receptor; Baculovirus; Sf9; Binding pharmacology

## 1. Introduction

Traditionally, glutamate receptors have been divided into two major groups, the ionotropic receptors which are ligand-gated ion channels permeable to cations and the metabotropic receptors which are G-protein coupled receptors (Hollmann and Heinemann, 1994). The ionotropic receptors are further divided into  $\alpha$ -amino-3-hydroxy-5-methyl-4-isoxazolepropionate (AMPA) receptors, kainate receptors and *N*-methyl-D-aspartate (NMDA) receptors, based upon pharmacological and electrophysiological data (Barnard, 1997). Ionotropic glutamate receptors (iGluRs) play an important role in the central nervous system (CNS) where they constitute the major excitatory transmitter system and are believed to be involved in various neuropathological conditions by a mediation of the excitotoxic action of glutamate (Choi, 1988; Beal, 1992; Whetsell, 1996).

Molecular cloning studies have shown that there are four AMPA receptor subunits, GluR1–4 (Hollmann and Heinemann, 1994), which are similar in size ( $\approx 900$  a.a.) and which share an amino acid sequence identity of about 65–70%. Each of these subunits can exist in a flip or flop version, created by alternative splicing of an 115 bp region of the mRNA (Sommer et al., 1990). Furthermore, RNA editing occurs for GluR2 resulting in a glutamine residue in the proposed ion pore-forming region being changed to an arginine residue. This RNA editing difference between GluR2 and the other AMPA receptor subunits influences the divalent cation permeability and the rectification properties of the channel (Sommer et al., 1991; Hume et al., 1991; Verdoorn et al., 1991; Sommer and Seeburg, 1992).

The AMPA receptor subunits co-assemble to form functional homomeric and heteromeric receptor channel complexes (Boulter et al., 1990; Keinänen et al., 1990) but the exact number of subunits and the stoichiometric composition of native AMPA receptors are still unclear. Biochemical (Hunter et al., 1990; Hunter and Wenthold, 1992; Wu

\* Corresponding author. Tel.: +45-35-37-67-77, ext. 277; Fax: +45-35-37-06-33; E-mail: picker@mail.dfh.dk.

and Chang, 1994) and functional (Ferrier-Montiel and Montal, 1996) experiments have suggested a pentameric AMPA channel structure similar to that of the GABA<sub>A</sub> receptor channel (Nayeem et al., 1994) or the nicotinic acetylcholine receptor channel (Unwin, 1993). However, functional studies on both the AMPA (Vodyanoy et al., 1993; Clements et al., 1998; Mano and Teichberg, 1998) and NMDA (Laube et al., 1998) channels suggest a tetrameric structure for the ionotropic glutamate receptors consisting of two distinct agonist binding sites. [<sup>3</sup>H]AMPA radioligand binding studies have shown that native AMPA receptors are not homogeneous and both high and low affinity binding sites are seen (Honoré et al., 1982; Murphy et al., 1987; Olsen et al., 1987; Honoré and Drejer, 1988; Giberti et al., 1991; Sawutz et al., 1995). Unfortunately, because of the heterogeneity of brain AMPA receptors the nature of these multiple sites cannot be determined. Binding experiments with membranes from recombinant AMPA receptor expression systems show only high affinity binding, indicating that the low affinity site is not detectable under these conditions. One exception is the GluR2 subunit where both high and low affinity sites have been shown (Andersen et al., 1996; Hennegriff et al., 1997). Despite these differences from native receptors, transfected cell lines can be helpful for biochemical and radioligand binding characterisation of the AMPA receptors.

Various expression systems have been established for studying the functional and pharmacological properties of the individual recombinant AMPA receptor subunits. Expression of these receptors in the baculovirus/Sf9 system (Kawamoto et al., 1991; Hattori et al., 1994; Keinänen et al., 1994; Kawamoto et al., 1994, 1995; Kuusinen et al., 1995) allows the production of large amounts of receptor, which is useful for radioligand binding experiments. In an attempt to compare previous pharmacological and electrophysiological data on homomeric and heteromeric GluR1<sub>0</sub> and GluR3<sub>0</sub> receptors (Banke et al., 1997) with their receptor binding pharmacology, recombinant baculoviruses carrying GluR1<sub>0</sub>, GluR3<sub>0</sub> and GluR1<sub>0</sub> + GluR3<sub>0</sub> were constructed. These were subsequently used for infection of *Spodoptera frugiperda* (Sf9) insect cells, providing membranes containing recombinant AMPA receptors for radioligand binding experiments, and the pharmacological properties were characterised using different AMPA agonists previously synthesised (Krogsgaard-Larsen et al., 1985; Madsen et al., 1992; Madsen and Wong, 1992).

## 2. Materials and methods

### 2.1. PCR mutagenesis

Rat GluR1<sub>0</sub> and GluR3<sub>0</sub> clones (in pBluescript vector) were provided by Dr. Stephen Heinemann (Salk Institute, CA). In order to create recombinant baculoviruses of these

clones, it was necessary to remove the 5'-untranslated sequence containing false start codons. Therefore, PCR mutagenesis was used to insert an *Eag*I restriction site 14 bases upstream of the start codon of GluR1<sub>0</sub> or six bases upstream from the start codon of GluR3<sub>0</sub>. The mutagenic primers used were: (for GluR1<sub>0</sub>), 3'-CGAAGAAAAA *gc*-CGcaACA-5' and 5'-GCTTCTTTT *cg*GCgtTGT-3'; (for GluR3<sub>0</sub>), 3'-TCGGgCCGgCTTCTTTTA-5' and 5'-AGCCcGGCcGAAGAAAAT-3' (Pharmacia BioTech, Sweden); where the *Eag*I site is in italics and mutagenic bases are indicated in lower case. PCR fragments were generated using the T3 and T7 primers for pBluescript along with the corresponding mutagenic primers. The PCR fragments generated using the T3 primer (≈ 0.3 kbp) were digested with *Xba*I and *Eag*I to give a 215 bp fragment (GluR1<sub>0</sub>) or a 190 bp fragment (GluR3<sub>0</sub>), while those from the T7 primer reaction (≈ 2.9 kbp) were digested with *Xho*I and *Eag*I to give a 2814 bp fragment (GluR1<sub>0</sub>) or a 2913 bp fragment (GluR3<sub>0</sub>). These digestion fragments were ligated together into the *Xba*I (5')–*Xho*I (3') site of pBSK(–) vector (Stratagene, CA). The 268 bp *Not*I–*Age*I fragment of this GluR1<sub>0</sub> construct was cassetted back into wild-type GluR1<sub>0</sub>pBSK(–) and the 195 bp *Xmn*I–*Eag*I fragment of the GluR3<sub>0</sub> construct cassetted into wildtype GluR3<sub>0</sub>pBSK(–). The sequence of these cassetted regions was verified by dideoxy sequencing (T7 Sequenase kit, Amersham, UK).

### 2.2. Construction of recombinant baculoviruses

The GluR1<sub>0</sub>(*Eag*I)pBSK(–) and GluR3<sub>0</sub>(*Eag*I)pBSK(–) constructs were digested with *Xho*I and blunt-ended with Klenow enzyme followed by digestion with *Eag*I and subsequent ligation into the *Eag*I (5')–*Sma*I (3') sites of the baculovirus transfer vector pVL1392 (PharMingen, CA), which places these sequences under the control of the baculoviral polyhedrin promoter. In order to study the heteromeric GluR1<sub>0</sub> + GluR3<sub>0</sub> receptor complex, a recombinant baculovirus was created which expresses both GluR1<sub>0</sub> and GluR3<sub>0</sub>. The GluR1<sub>0</sub>(*Eag*I)pBSK(–) construct was digested with *Eag*I and *Xho*I, blunt-ended with Klenow enzyme and ligated into the *Bam*HI site (also blunt-ended) of the baculovirus transfer vector pAcUW51 (PharMingen, CA). The GluR3<sub>0</sub>(*Eag*I)pBSK(–) construct was digested with *Eag*I and *Sph*I, blunt-ended with Klenow enzyme and ligated into the *Bgl*II (blunt-ended) site of pAcUW51. The resulting construct, (GluR1<sub>0</sub> + GluR3<sub>0</sub>)pAcUW51, contained GluR1<sub>0</sub> under control of the baculoviral polyhedrin promoter and GluR3<sub>0</sub> under control of the baculoviral p10 promoter. These final constructs: GluR1<sub>0</sub>pVL1392, GluR3<sub>0</sub>pVL1392 and (GluR1<sub>0</sub> + GluR3<sub>0</sub>)pAcUW51 were used in conjunction with the BaculoGold transfection kit (PharMingen, CA) to create recombinant GluR1<sub>0</sub>, GluR3<sub>0</sub> and GluR1<sub>0</sub> + GluR3<sub>0</sub> baculoviruses.

### 2.3. Recombinant baculovirus production and cell culture

All manipulations of the virus and maintenance of the insect cells were according to standard protocols in 'Guide to Baculovirus Expression Vector Systems (BEVS) and Insect Cell Culture Techniques', (Gibco, UK). Plaque purification was used to isolate recombinant viruses, followed by serial amplification to obtain high titre virus stocks. The virus stocks were checked by PCR and receptor expression of infected cells was monitored by western immunoblotting. Virus titre was determined by plaque assay. Sf9 cells were maintained at 27°C in suspension culture in 100–1000 ml disposable spinner flasks (Corning Costar, MA) using Sf-900 II serum free medium (Gibco, UK) supplemented with penicillin (50 units/ml) and streptomycin (50 µg/ml). Suspension cultures with a density of  $1\text{--}2 \times 10^6$  cells/ml were infected with recombinant baculovirus at a multiplicity of infection (MOI) of 10 by adding the virus stock directly to the suspension culture. The cells were infected for 60–65 h and harvested by centrifugation ( $500 \times g$ , 10 min, 4°C), followed by an homogenisation and washing step. For preparation of membranes, the cell pellet from  $\approx 1000$  ml culture was resuspended in 0.2 culture volumes of ice cold 50 mM Tris-HCl buffer pH 7.4 (at 4°C) supplemented with protease inhibitors (1 mM EDTA, 0.1 mM PMSF, 10 µg/ml turkey egg white trypsin inhibitor, 1 µg/ml aprotinin, 10 µg/ml leupeptin, 1 mM (D,L)-benzylsuccinate, 1 mM L-leucine hydroxamate, 50 units/ml bacitracin) with an Ultra-Turrax tissue homogeniser and centrifuged at  $48,000 \times g$ , at 4°C for 30 min. The membrane pellet was washed once more in this buffer and then washed thrice more using this buffer without the protease inhibitors. The final washed membrane pellet was stored at  $-80^\circ\text{C}$  in aliquots until used for experiments.

### 2.4. Radioligand binding assay

(*R,S*)-[ $^3\text{H}$ ]AMPA equilibrium binding to membranes containing GluR1<sub>o</sub>, GluR3<sub>o</sub> or GluR1<sub>o</sub> + GluR3<sub>o</sub> was performed (in triplicate) in a final volume of 250 µl, with 50–300 µg of membrane protein per assay tube, using typically 5–10 nM (*R,S*)-[ $^3\text{H}$ ]AMPA (45.3–53.1 Ci/mmol) in an assay buffer containing: 50 mM Tris-HCl, 100 mM KSCN and 2.5 mM CaCl<sub>2</sub>, pH 7.2, (Murphy et al., 1987; Honoré and Drejer, 1988). Preliminary binding experiments indicated a linear response of specific binding over this range of protein concentration. Incubations were carried out on ice for 90 min and were terminated by rapid filtration through Whatman GF/B filters on a 48-well cell harvester (Brandel, MD), or using a 12-well Millipore filtration manifold for kinetic experiments. Filters were pre-treated with 0.3% polyethyleneimine (PEI) in 50 mM Tris base for 2–3 h before use. After sample filtration, filters were washed with  $3 \times 5$  ml of 4°C assay buffer and radioactivity determined by liquid scintillation counting in

4 ml Ecoscint A (National Diagnostics, Atlanta, GA) in a Packard 2000CA scintillation counter. Non-specific binding was determined in the presence of 1 mM L-glutamate and was subtracted from total binding to obtain specific binding. The non-specific binding generally represented 5–10% of total binding and was linear over the radioligand concentration range used.

For saturation binding, membranes were incubated with 1–300 nM (*R,S*)-[ $^3\text{H}$ ]AMPA, adjusted to a specific activity of 15–20 Ci/mmol with unlabeled (*R,S*)-AMPA. Ligand competition assays were carried out at a fixed label concentration and a range ( $10^{-10}$ – $10^{-3}$  M) of unlabelled ligand. Kinetic experiments were performed with 5–10 nM (*R,S*)-[ $^3\text{H}$ ]AMPA (10–53.1 Ci/mmol) and for association kinetics, the membranes were incubated with (*R,S*)-[ $^3\text{H}$ ]AMPA for 0.5 min to 3 h before filtration. The dissociation experiments were initiated by adding an excess (1 mM) of L-glutamate after steady state conditions had been achieved and then filtering the samples at times from 0.25–30 min. All drugs for the competition assays were stored at  $-80^\circ\text{C}$  in 10 mM stock solutions, dissolved in assay buffer (without KSCN) or in DMSO ( $\leq 30\%$ )–water (CNQX and NBQX).

### 2.5. Electrophoresis and immunoblotting

Protein determinations were made using the micro bicinchoninic acid protein assay (Pierce Chemicals, IL) with bovine serum albumin as the standard. *N*-glycosidase F treatment of GluR1<sub>o</sub> and GluR3<sub>o</sub> receptors expressed in Sf9 cell membranes was performed overnight at 37°C under conditions recommended by the manufacturer (Boehringer Mannheim). Samples were subjected to (8–10% resolving gel) discontinuous sodium dodecyl sulphate polyacrylamide gel electrophoresis (SDS-PAGE) according to Laemmli (1970) and western transfer was performed onto nitrocellulose membranes (Millipore, MA). Receptor bands were visualised using rabbit polyclonal anti-rat GluR1 antibody (1 µg/ml), or anti-rat GluR2/3 antibody (1 µg/ml), and goat anti-rabbit IgG(Fc)-alkaline phosphatase conjugated secondary antibody followed by NBT/BCIP substrate colour development.

### 2.6. Data analysis

The non-linear curve-fitting programme Grafit v3.0 (Erithacus Software, UK) was used for the analysis of binding data. Specific binding from saturation experiments was fit to both a one or two site model without ligand depletion being taken into consideration (Eq. (1)), or a one site model considering ligand depletion (Eq. (2); see Hulme and Birdsall, 1992). IC<sub>50</sub> values and Hill coefficients ( $n_H$ ) were determined from inhibition experiments analysed by the four parameter logistic equation (Eq. (3)).  $K_i$  values were obtained by fitting inhibition data to Eq. (4), using a one site model.  $K_d$  and  $B_{\max}$  at the heteromeric receptor

complex were derived from competition experiments, where  $(R,S)$ -[ $^3$ H]AMPA binding was displaced by unlabeled  $(R,S)$ -AMPA and the  $K_d$  value derived from Eq. (4) by setting  $K_i = K_d$ . Dissociation experiments were analysed by fitting the total binding to mono- and bi-exponential rate equations (Eq. (5)). Association experiments were analysed by fitting the specific binding to mono and bi-exponential rate equations without ligand depletion considered (Eq. (6)) or a one site model considering ligand depletion (Eq. (7)). Apparent rate constants were determined by fitting association binding data to Eq. (8). The  $F$ -test was used to determine which model best fitted the data. Student's  $t$ -test was used to compare  $K_i$  values. In all statistical tests  $P \leq 0.05$  was considered significant. All results are given as mean  $\pm$  S.D.

## 2.7. Equations<sup>1</sup>

$$\sum_i B_{\max_i} \cdot L_f / (K_{d_i} + L_f) \quad (1)$$

$$0.5 \cdot \left[ L_t + K_d + B_{\max} - \left\{ (L_t + K_d + B_{\max})^2 - 4 \cdot B_{\max} \cdot L_t \right\}^{1/2} \right] \quad (2)$$

$$TB_{\max} / \left( 1 + ([I]/IC_{50})^{n_H} \right) + NSB \quad (3)$$

$$\sum_i (R_{t_i} \cdot L_t / K_{d_i}) / \left( 1 + L_t / K_{d_i} + [I] / K_{i_i} \right) + NSB \quad (4)$$

$$\sum_i RL_{o_i} \cdot \exp(-k_{off_i} \cdot t) + NSB \quad (5)$$

$$\sum_i RL_{eq_i} \cdot \left[ 1 - \exp(-k_{on_i} \cdot L_f \cdot t - k_{off_i} \cdot t) \right] \quad (6)$$

$$(RL_{eq} \cdot b) (\exp(c) - 1) / (RL_{eq} \cdot \exp(c) - b),$$

where:  $b = R_t \cdot L_t / RL_{eq}$ ,  $c = (RL_{eq} - b) \cdot k_{on} \cdot t$  (7)

$$\sum_i RL_{eq_i} \cdot \left[ 1 - \exp(-k_{app_i} \cdot t) \right] \quad (8)$$

## 2.8. Drugs and reagents

$(R,S)$ -2-amino-3-hydroxy-5-methyl-4-isoxazolepropionate (AMPA),  $(R,S)$ -2-amino-3-(3-carboxy-5-methyl-

4-isoxazolyl)propionate (ACPA) and  $(R,S)$ -2-amino-3-(3-hydroxy-5-trifluoromethyl-4-isoxazolyl)propionate (Tri-F-AMPA) were synthesised in the Department of Medicinal Chemistry, The Royal Danish School of Pharmacy

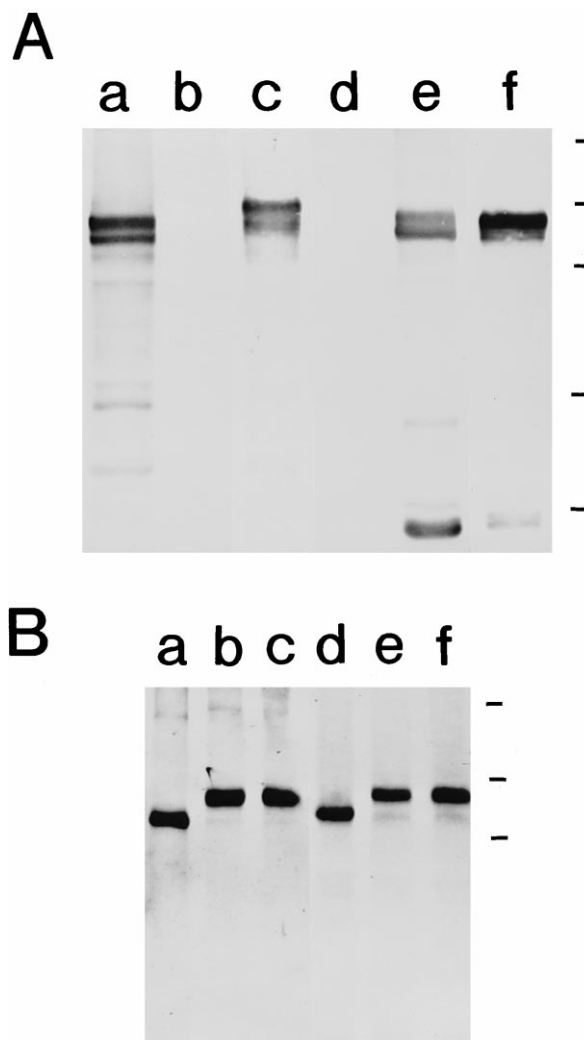


Fig. 1. Western immunoblots of Sf9 membranes containing recombinant rat AMPA receptors. Membranes of infected Sf9 cells were prepared and analysed by SDS-PAGE and western immunoblotting as described in Section 2. Panel A (10% gel): lanes a and d, GluR1<sub>o</sub>; lanes b and e, GluR3<sub>o</sub>; lanes c and f, heteromeric GluR1<sub>o</sub> + 3<sub>o</sub>. Lanes a–c were developed with the anti-GluR1 antibody, while lanes d–f were developed with the anti-GluR2/3 antibody. A doublet of bands is seen for both receptors (kDa, mean  $\pm$  S.D.,  $n = 4$ ): GluR1<sub>o</sub>,  $109 \pm 3$  and  $100 \pm 4$ ; GluR3<sub>o</sub>,  $108 \pm 1$  and  $99 \pm 2$ . Deglycosylation of the receptors by  $N$ -glycosidase F treatment is indicated in panel B (8% gel): lanes a–c, GluR1<sub>o</sub>; lanes d–f, GluR3<sub>o</sub>. Lanes a and d: with enzyme and 37°C incubation; lanes b and e, without enzyme but with 37°C incubation; lanes c and f, without enzyme or 37°C incubation. Deglycosylation shifts all of the upper band down to the lower band for both receptors, with a loss of  $\approx 9$  kDa in each case. Each lane in panels A and B was loaded with 2–3  $\mu$ g protein. Positions of molecular mass markers is indicated on the right of panels A and B; from top to bottom (kDa): 200, 113, 82, 49.2 34.8.

<sup>1</sup>  $B_{\max_i}$  =  $i$ th binding site concentration,  $K_{d_i}$  = radioligand dissociation constant at the  $i$ th binding site,  $K_{i_i}$  = inhibitor dissociation constant at the  $i$ th binding site,  $RL_{o_i}$  = total bound ligand at time zero to the  $i$ th binding site,  $RL_{eq_i}$  = equilibrium total binding at the  $i$ th binding site,  $t$  = time,  $k_{on_i}$  = association rate constant of the radioligand at the  $i$ th binding site,  $k_{off_i}$  = dissociation rate constant of the radioligand at the  $i$ th binding site,  $k_{app_i}$  = apparent rate constant of the radioligand at the  $i$ th binding site,  $L_t$  = total radioligand concentration,  $L_f$  = free radioligand concentration,  $TB_{\max}$  = total radioligand bound at zero competitor concentration,  $IC_{50}$  = inhibitor concentration producing 50% specific binding,  $n_H$  = Hill coefficient, NSB = non-specific binding,  $[I]$  = total competitive inhibitor concentration. (For a more complete description of the equations used, see Hulme and Birdsall, 1992).

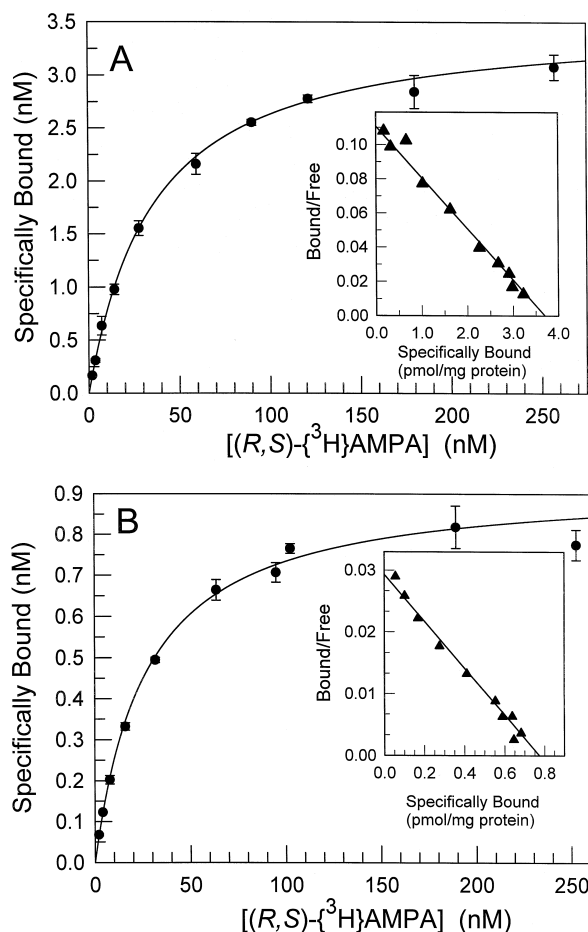


Fig. 2. Saturation binding curves and Scatchard plots (insets) for (panel A) GluR1<sub>o</sub> and (panel B) GluR3<sub>o</sub>, from representative experiments, repeated twice. Data points are the mean  $\pm$  S.D. specific binding of triplicate samples and were fit to Eq. (1). (R,S)-[<sup>3</sup>H]AMPA was incubated with Sf9 membranes containing GluR1<sub>o</sub> or GluR3<sub>o</sub> as described in Section 2 and non-specific binding defined as that binding remaining in the presence of 1 mM L-glutamate. GluR1<sub>o</sub>:  $K_d = 33.4$  nM,  $B_{max} = 3.70$  pmol/mg protein; GluR3<sub>o</sub>:  $K_d = 26.5$  nM,  $B_{max} = 0.94$  pmol/mg protein. (See Table 1 for average  $K_d$  and  $B_{max}$  values).

Table 1

Ligand binding properties of homomeric and heteromeric GluR1<sub>o</sub> and GluR3<sub>o</sub> AMPA receptors expressed in Sf9 cells

Drug	GluR1 <sub>o</sub>		GluR3 <sub>o</sub>		GluR1 <sub>o</sub> + GluR3 <sub>o</sub>	
	$K_i$ (nM)	$n_H$	$K_i$ (nM)	$n_H$	$K_i$ (nM)	$n_H$
Tri-F-AMPA	$21.4 \pm 2.3^{a,b}$	$0.98 \pm 0.06$	$9.7 \pm 0.9^d$	$1.03 \pm 0.12$	$10.0 \pm 4.7$	$0.93 \pm 0.14$
AMPA	$29.9 \pm 4.5^{a,b}$	$0.98 \pm 0.13$	$19.2 \pm 2.7^d$	$0.99 \pm 0.17$	$16.6 \pm 4.2$	$0.91 \pm 0.07$
ACPA	$45.1 \pm 3.1^{a,b}$	$0.95 \pm 0.09$	$15.5 \pm 3.1^d$	$0.94 \pm 0.04$	$15.3 \pm 2.7$	$0.91 \pm 0.05$
L-glutamate	$169 \pm 27$	$0.93 \pm 0.10$	$249 \pm 12$	$1.10 \pm 0.05$	$153 \pm 25$	$0.92 \pm 0.17$
NBQX	$207 \pm 13$	$1.10 \pm 0.12$	$174 \pm 21$	$0.94 \pm 0.09$	$274 \pm 97$	$0.88 \pm 0.10$
CNQX	$263 \pm 17$	$0.96 \pm 0.08$	$513 \pm 62$	$0.89 \pm 0.02$	$223 \pm 28$	$0.94 \pm 0.02$
Kainate	$477 \pm 76^c$	$0.85 \pm 0.02$	$1980 \pm 340^c$	$0.94 \pm 0.07$	$623 \pm 23^c$	$0.98 \pm 0.10$
$K_d$ (nM) (saturation)	$32.5 \pm 2.7$		$23.7 \pm 2.7$		$18.1 \pm 2.9^*$	
$B_{max}$ (pmol/mg protein)	$3.75 \pm 0.63$		$0.81 \pm 0.16$		$1.29 \pm 0.08^*$	

All values are the mean  $\pm$  S.D. from 3–4 experiments.

<sup>a,c</sup> Significantly different from one another by the *t*-test ( $P < 0.05$ ).

<sup>b</sup> Tri-F-AMPA, AMPA and ACPA  $K_i$  values at GluR1<sub>o</sub> are significantly different from their GluR3<sub>o</sub> or GluR1<sub>o</sub> + GluR3<sub>o</sub>  $K_i$  values, which were not significantly different from each other.

<sup>d</sup> Tri-F-AMPA significantly different from AMPA or ACPA at GluR3<sub>o</sub>.

\* Values were determined from competition experiments by displacing (R,S)-[<sup>3</sup>H]AMPA by unlabeled (R,S)-AMPA.

(Krogsgaard-Larsen et al., 1985; Madsen and Wong, 1992; Madsen et al., 1992). Kainate, *N*-methyl-D-aspartate (NMDA), 6-cyano-7-nitroquinoxaline-2,3-dione (CNQX) and 6-nitro-7-sulphamoylbenzo[*f*]quinoxaline-2,3-dione (NBQX) were purchased from Tocris Cookson (UK). Rabbit polyclonal anti-rat GluR1 and GluR2/3 antibodies were from UBI (Lake Placid, NY). Goat anti-rabbit IgG(F<sub>c</sub>)-alkaline phosphatase conjugated antibody and NBT/BCIP substrate were from Promega (Madison, WI). (R,S)-[5-methyl-<sup>3</sup>H]AMPA (45.3–53.1 Ci/mmol) was purchased from Du Pont-New England Nuclear (Wilmington, DE). Restriction enzymes and other molecular biological enzymes were obtained from New England BioLabs (Beverly, MA). Other drugs and reagents were from Sigma (St. Louis, MO) or similar commercial suppliers.

### 3. Results

#### 3.1. Virus production and receptor expression

During the viral amplification procedure, Sf9 cells infected with the recombinant baculoviruses containing rat GluR1<sub>o</sub> and GluR3<sub>o</sub> were lysed and analysed by PCR using GluR1 or GluR3 specific primers to confirm the nature of the virus being amplified and western immunoblots of the membranes indicated correct subunit expression (data not shown). The time course of GluR1<sub>o</sub> and GluR3<sub>o</sub> expression in Sf9 cells was followed by infecting a suspension culture of cells and removing aliquots at different time points to be assayed for (R,S)-[<sup>3</sup>H]AMPA binding activity. Significant binding was observed after 24 h infection and the maximum was reached around 70 h, followed by a gradual decrease until 120 h (data not shown). From these observations, it was decided to use an infection time of 60–65 h for production of Sf9 membranes containing these receptors.

### 3.2. Western immunoblots and receptor deglycosylation

Membranes from Sf9 cells expressing homomeric and heteromeric GluR1<sub>o</sub> and GluR3<sub>o</sub> receptors were subjected to SDS-PAGE and western immunoblotting (Fig. 1A,B). GluR1<sub>o</sub>-, GluR3<sub>o</sub>- and GluR1<sub>o</sub> + GluR3<sub>o</sub>-containing membranes produced a doublet of immunoreactive protein bands at  $M_r = 109 \pm 3$  and  $100 \pm 4$  kDa (GluR1<sub>o</sub>) or  $M_r = 108 \pm 1$  and  $99 \pm 2$  kDa (GluR3<sub>o</sub>), which likely correspond to the glycosylated and unglycosylated forms of the proteins. Moreover, membranes from wild-type infected and non-infected Sf9 cells did not yield any immunoreactive bands

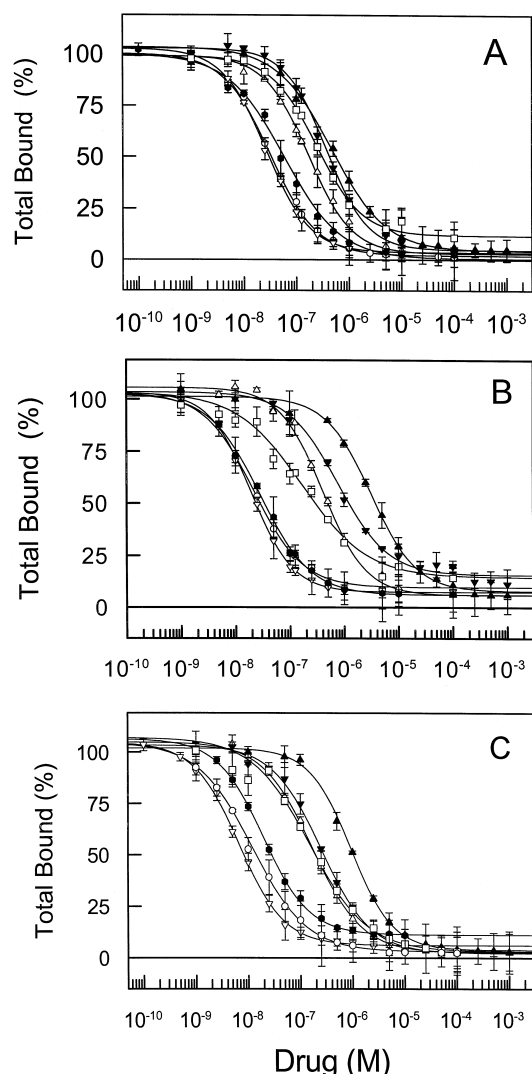


Fig. 3. Inhibitor binding pharmacology at: (panel A) homomeric GluR1<sub>o</sub>, (panel B) homomeric GluR3<sub>o</sub> and (panel C) heteromeric GluR1<sub>o</sub> + 3<sub>o</sub> receptors. Inhibitors were incubated with 5–10 nM (*R,S*)-[<sup>3</sup>H]AMPA and assayed as described in Section 2. Each curve is a representative experiment (replicated 2–3 times) where the total binding (nM) was fit to a one site model (Eq. (4)) to determine  $K_i$ ,  $R_i$  and NSB for each curve.  $R_i$  was then set as the 100% value for that curve. Data points are the mean  $\pm$  %S.D. of triplicate samples: Tri-F-AMPA ( $\nabla$ ), AMPA ( $\circ$ ), ACPA ( $\bullet$ ), L-glutamate ( $\Delta$ ), NBQX ( $\square$ ), CNQX ( $\blacktriangledown$ ), kainate ( $\blacktriangle$ ). (See Table 1 for average  $K_i$  and  $n_H$  values).

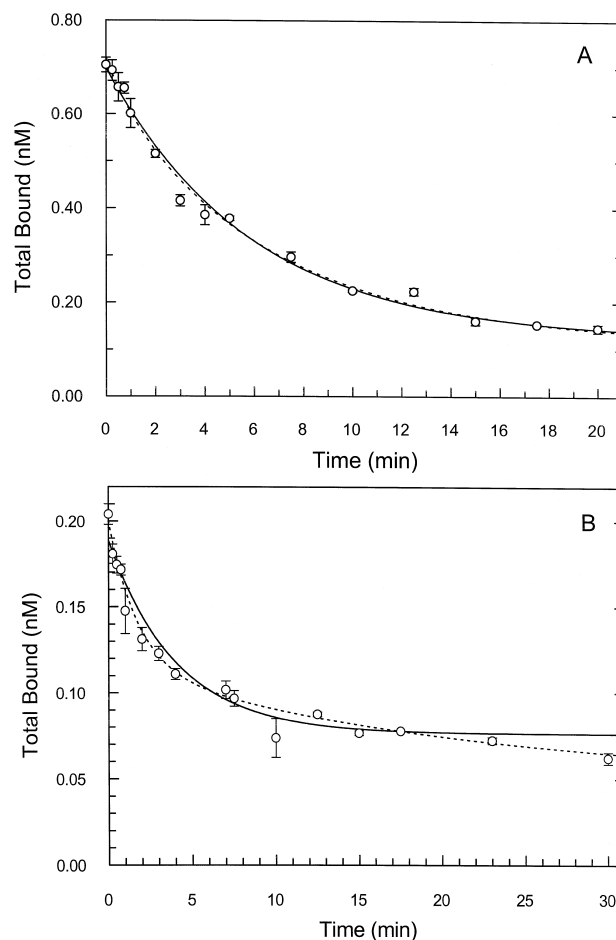


Fig. 4. Dissociation kinetics of (*R,S*)-[<sup>3</sup>H]AMPA binding to Sf9 membranes containing GluR1<sub>o</sub> (panel A) or GluR3<sub>o</sub> (panel B). The data were fit to a one (—) and two (---) site model using Eq. (5). For both experiments shown, a bi-exponential fit was not significantly better than a mono-exponential fit to the data. However, in one of the three GluR3<sub>o</sub> dissociation experiments performed, a bi-exponential fit was possible. Panels A and B represent single experiments (repeated 2–3 times) where each data point is the mean  $\pm$  S.D. of triplicate samples. Single site fit: GluR1<sub>o</sub>,  $k_{off} = 0.1716 \text{ min}^{-1}$ ; GluR3<sub>o</sub>,  $k_{off} = 0.2480 \text{ min}^{-1}$ . Two site fit: GluR1<sub>o</sub>,  $k_{off1} = 0.9391 \text{ min}^{-1}$ ,  $k_{off2} = 0.1535 \text{ min}^{-1}$ ; GluR3<sub>o</sub>,  $k_{off1} = 0.5776 \text{ min}^{-1}$ ,  $k_{off2} = 0.04906 \text{ min}^{-1}$ . (See Table 2 for average dissociation rate constants).

(data not shown). Treatment of homomeric GluR1<sub>o</sub> or GluR3<sub>o</sub> membranes with *N*-glycosidase F, which removes N-linked oligosaccharide side chains (Tarentino et al., 1985), resulted in a disappearance of the upper band and an increase in intensity of the lower band (Fig. 1B). This confirmed that each of the AMPA receptor subunits expressed in these Sf9 cells produces two distinct bands on western blots, corresponding to the glycosylated and unglycosylated forms of the receptor.

### 3.3. Saturation binding

Equilibrium binding studies with membranes expressing AMPA subunits were performed using (*R,S*)-[<sup>3</sup>H]AMPA.

Saturation experiments were conducted on homomeric GluR1<sub>o</sub> or GluR3<sub>o</sub> containing membranes and a single class of binding site was detected for GluR1<sub>o</sub>:  $K_d = 32.5 \pm 2.7$  nM,  $B_{max} = 3.75 \pm 0.63$  pmol/mg protein,  $n = 4$  (Fig. 2A and Table 1); and for GluR3<sub>o</sub>:  $K_d = 23.7 \pm 2.4$  nM,  $B_{max} = 0.81 \pm 0.16$  pmol/mg protein,  $n = 4$  (Fig. 2B and Table 1). The radioligand dissociation constant ( $K_d = 18.1 \pm 2.9$  nM) and an estimate of receptor density ( $B_{max} = 1.29 \pm 0.08$  pmol/mg protein) for the heteromeric receptor complex were derived from competition experiments ( $n = 4$ ), where (R,S)-[<sup>3</sup>H]AMPA binding was displaced by unlabeled (R,S)-AMPA (see Fig. 3C).

Attempts were made to fit the saturation data to a two site model, but this was not statistically significantly better than a one-site fit (by *F*-test). In addition, the data were fit to a single site model which accounted for ligand depletion effects, but this produced fits which were not statistically significantly different from the 'non-depletion' single site model, indicating that ligand depletion is not problematic in these experiments. Scatchard transformation of the saturation data yielded linear plots (insets: Fig. 2A,B), indicating the presence of a single binding site population for GluR1<sub>o</sub> and GluR3<sub>o</sub>.

### 3.4. Kinetic experiments

Dissociation of (R,S)-[<sup>3</sup>H]AMPA binding to membranes containing GluR1<sub>o</sub> was best fit, as determined by the *F*-test, to a mono-exponential equation (Eq. (5)) giving one rate constant ( $k_{off}$ ) (Fig. 4A, Table 2). Yet, for GluR3<sub>o</sub>, one of three dissociation experiments was significantly better fit using a bi-exponential rate equation (Eq. (5)) (Fig. 4B, Table 2). For both receptors, the corresponding radioligand association kinetic experiments yielded a better fit to a bi-exponential equation (Eq. (8)) than a mono-exponential equation (Eq. (6)) (Fig. 5A and B, Table

Table 2

Kinetic rate constants for binding of (R,S)-[<sup>3</sup>H]AMPA to homomeric GluR1<sub>o</sub> and GluR3<sub>o</sub> receptors

Rate constants	GluR1 <sub>o</sub>	GluR3 <sub>o</sub>
<i>Single rate model</i>		
$k_{off}$ (min <sup>-1</sup> )	$0.2013 \pm 0.0676$	$0.1913 \pm 0.0582$
$k_{on}$ (nM <sup>-1</sup> min <sup>-1</sup> )	$0.005428 \pm 0.003139$	$0.02402 \pm 0.00749$
$k_{off}/k_{on} = K_d$	37 nM	8.0 nM
<i>Double rate model</i>		
$k_{off1}$ (min <sup>-1</sup> )	$0.8256 \pm 0.4913$	$0.5842 \pm 0.1465$
$k_{off2}$ (min <sup>-1</sup> )	$0.1329 \pm 0.0259$	$0.05608 \pm 0.00994$
$k_{app1}$ (min <sup>-1</sup> )	$0.9343 \pm 0.4231$	$0.8988 \pm 0.3712$
$k_{app2}$ (min <sup>-1</sup> )	$0.09659 \pm 0.05285$	$0.03411 \pm 0.03780$

For the dissociation kinetics,  $P > 0.05$  for the double rate model vs. the single rate model with GluR1<sub>o</sub> (by *F*-test), but with GluR3<sub>o</sub>, one of three experiments gave a better fit to the double rate model.

For the association kinetics, all experiments were statistically significantly ( $P < 0.05$ ) better fit to a double rate model than to a single rate model. However, it was not possible to isolate the individual  $k_{on1}$  and  $k_{on2}$  values. GluR1<sub>o</sub>,  $n = 4$ ; GluR3<sub>o</sub>,  $n = 3$ .

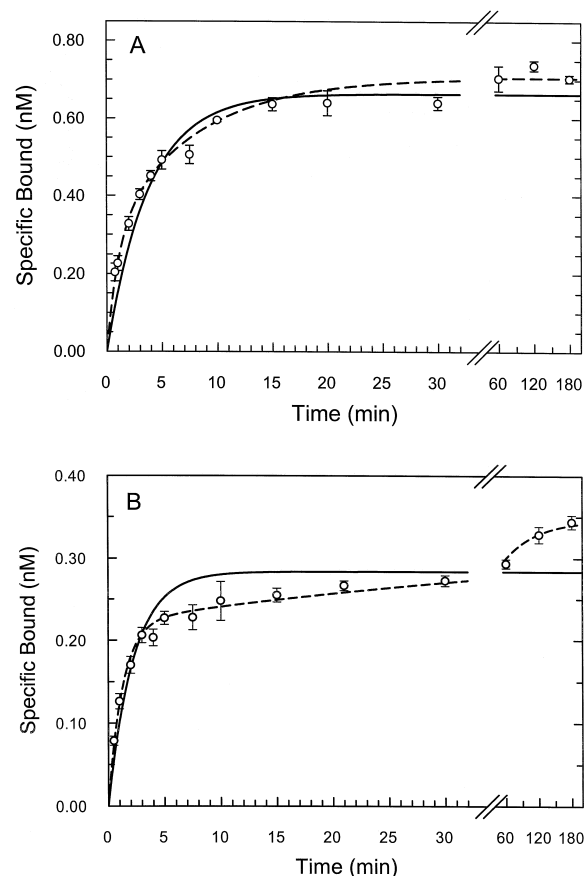


Fig. 5. Association kinetics of (R,S)-[<sup>3</sup>H]AMPA binding to Sf9 membranes containing GluR1<sub>o</sub> (panel A) or GluR3<sub>o</sub> (panel B). The data were fit to a one site model using Eq. (6) (—) or a two site model using Eq. (8) (---). A bi-exponential equation gave a significantly better fit than a mono-exponential equation for both GluR1<sub>o</sub> and GluR3<sub>o</sub>. Panels A and B represent single experiments (repeated 2–3 times) where each data point is the mean  $\pm$  S.D. of triplicate samples. Single site fit: GluR1<sub>o</sub>,  $k_{on} = 0.005876$  min<sup>-1</sup> nM<sup>-1</sup>; GluR3<sub>o</sub>:  $k_{on} = 0.02131$  min<sup>-1</sup> nM<sup>-1</sup>. Two site fit: GluR1<sub>o</sub>,  $k_{app1} = 0.9566$  min<sup>-1</sup>,  $k_{app2} = 0.1307$  min<sup>-1</sup>; GluR3<sub>o</sub>,  $k_{app1} = 0.7938$  min<sup>-1</sup>,  $k_{app2} = 0.01646$  min<sup>-1</sup>. (See Table 2 for average association rate constants).

2). However, attempts to isolate the individual association rate constants ( $k_{on1}$  and  $k_{on2}$ ) from the apparent rate constants ( $k_{app1}$  and  $k_{app2}$ ) by using the relation:  $k_{on} = (k_{app} - k_{off})/L_t$ , were unsuccessful. A fit of the association kinetic data to a mono-exponential equation which also accounted for ligand depletion (Eq. (7)) did not produce a significantly better fit than the 'non-depletion' mono-exponential equation, which again indicated that ligand depletion is not a problem in these kinetic studies. A calculation of  $K_d$  from the single  $k_{on}$  and  $k_{off}$  rates determined from the mono-exponential fits of the dissociation and association data gave: GluR1<sub>o</sub>,  $K_d = 37$  nM; GluR3<sub>o</sub>,  $K_d = 8.0$  nM (Table 2).

### 3.5. Inhibition experiments

The pharmacological profiles of a select number of compounds were determined at homomeric GluR1<sub>o</sub>, ho-

omeric GluR3<sub>o</sub> and at heteromeric GluR1<sub>o</sub> + GluR3<sub>o</sub> receptors (Fig. 3, Table 1). In all instances, the Hill values were unity, indicating the presence of a single population of binding sites for these receptors under these assay conditions and attempts to fit the inhibition data to multiple sites (Eq. (4)) failed. For homomeric GluR1<sub>o</sub> and GluR3<sub>o</sub>, as well as the heteromeric receptor complex, the rank order of drug affinities was similar: AMPA analogues > L-glutamate > quinoxaline-2,3-diones > kainate; the only exception being L-glutamate at homomeric GluR3<sub>o</sub>, where it has slightly lower affinity than NBQX. NMDA and L-aspartate had negligible affinity for these receptors (data not shown).

#### 4. Discussion

In an effort to characterise the agonist binding site of the AMPA receptor and identify possible subtype-selective agonists, the functional potencies (EC<sub>50</sub>'s) of AMPA analogues at recombinant rat GluR1<sub>o</sub> and GluR3<sub>o</sub> receptors expressed in the *Xenopus* oocyte have recently been examined (Banke et al., 1997). One AMPA analogue studied, (*R,S*)-2-amino-3-(3-carboxy-5-methyl-4-isoxazolyl)propionate (ACPA), was found to exhibit an  $\approx 11$ -fold selectivity for GluR3<sub>o</sub> over GluR1<sub>o</sub>. In order to further examine this subtype selective agonist, the present study has evaluated the radioligand binding pharmacology of these AMPA analogues at homomeric and heteromeric GluR1<sub>o</sub> and GluR3<sub>o</sub> receptors produced in the Sf9 insect cell expression system.

The expression of both GluR1<sub>o</sub> and GluR3<sub>o</sub> subunits observed in this study compared favourably with previous reports regarding AMPA receptor subunits expressed in insect cells (Kawamoto et al., 1994; Keinänen et al., 1994; Kuusinen et al., 1995). The expression level was high, non-specific (*R,S*)-[<sup>3</sup>H]AMPA radioligand binding low and the pharmacological profile typical for the AMPA-selective ionotropic glutamate receptors (see below). Furthermore, the time course of expression showed significant binding after 24 h of infection and maximal levels around 70 h post-infection which is in agreement with previous reports (Kawamoto et al., 1991; Keinänen et al., 1994; Hattori et al., 1994). Western immunoblotting of membrane samples containing the homomeric or heteromeric receptors indicated the characteristic double band pattern (99–109 kDa) corresponding to the glycosylated and unglycosylated forms, or to differentially glycosylated forms, of the receptor subunits. These results are in good accord with previous reports of expression of recombinant AMPA subunits which have revealed a doublet of bands of  $\approx 106/104$  kDa and  $102/98$  kDa (Kawamoto et al., 1994; Hattori et al., 1994; Kawamoto et al., 1995; Hall et al., 1997). Western immunoblots of native brain GluR1–4 subunits have generally revealed a single band of  $\approx 108$  kDa (Wentholt et al., 1992; Blackstone et al., 1992). The

observation of a receptor band doublet in insect cell expression systems, compared to a single band which is usually seen with native receptor, can be explained by the fact that over-expression of these proteins in the insect cells by baculoviral promoter sequences causes accumulation of a large intracellular pool of receptor which is not glycosylated. Indeed, deglycosylation of GluR1<sub>o</sub> and GluR3<sub>o</sub> subunits from Sf9 membranes by *N*-glycosidase F, which removes all N-linked carbohydrate residues (Tarentino et al., 1985), caused a loss of  $\approx 9$  kDa in mass from the upper band for both subunits, shifting them down to the size of the lower band. The measured sizes of the deglycosylated bands correspond with the calculated *M<sub>r</sub>* values deduced from the cDNA sequences for GluR1<sub>o</sub> (99.8 kDa) and GluR3<sub>o</sub> (98.0 kDa).

Previous studies of (*R,S*)-[<sup>3</sup>H]AMPA binding to brain tissue have indicated the presence of two affinity sites which correspond to a high and low affinity site (Honoré et al., 1982; Murphy et al., 1987; Honoré and Drejer, 1988; Giberti et al., 1991; Hunter et al., 1990; Sawutz et al., 1995). It has been proposed that this finding is a matter of a single interconvertible receptor population (Hall et al., 1992), corresponding to high affinity desensitised and low affinity non-desensitised states. The chaotropic agent potassium thiocyanate is thought to influence (*R,S*)-[<sup>3</sup>H]AMPA binding by enhancing binding to the high affinity, desensitised receptor state (Honoré and Drejer, 1988; Nielsen et al., 1988; Hall et al., 1993a). In addition, it has been shown in electrophysiological experiments that potassium thiocyanate has an influence on the channel properties by increasing the extent and rate of onset of desensitisation, suggesting that AMPA receptors are in a high affinity and desensitised form in the presence of potassium thiocyanate (Arai et al., 1995). It also seems to be the case that when the recombinant receptor subunits are expressed in non-neuronal cells they are mostly of the high affinity type, with the exception of the GluR2 subunit (Andersen et al., 1996; Hennegriff et al., 1997), where a low affinity site has been observed in transfected HEK293 cells. This implies that these AMPA receptors are predominantly in the desensitised state (Hall et al., 1993b).

In this study, saturation experiments showed one high affinity binding site for both homomeric and heteromeric receptors which is in good correspondence with observations from other studies employing insect cell expression systems (Kawamoto et al., 1994; Keinänen et al., 1994; Hattori et al., 1994; Kuusinen et al., 1995) or mammalian cells (Andersen et al., 1996; Hennegriff et al., 1997). So, either the low affinity, non-desensitised receptor state is not present, or it represents a very small portion of the total receptor population expressed in Sf9 membranes. As discussed above, the inclusion of potassium thiocyanate in the assay buffer enhances the binding to the high affinity state, perhaps shifting the equilibrium of the receptor population far away from the low affinity, non-desensitised state. Alternatively, the failure to observe the low affinity

site could be due to the inherent technical limitations of the radioligand filtration assay. Binding to a low affinity site could be lost during filtration due to rapid dissociation of the receptor–ligand complex.

Whilst the kinetics of  $(R,S)$ - $[^3H]$ AMPA dissociation from GluR1<sub>o</sub> and GluR3<sub>o</sub> were monophasic, the corresponding ligand association kinetics indicated biphasic kinetics, suggesting the presence of a second site which was not detected in equilibrium binding experiments. Since biphasic association kinetics are seen, and if this is due to the presence of a second binding site, it could be expected that biphasic dissociation kinetics should also be observed. This seeming incongruity could be explained by the presence of a second extremely fast  $k_{off}$  rate which is not detectable using a filtration assay or, alternatively, the second  $k_{off}$  rate could be similar or identical to the first  $k_{off}$  rate, in which case they could not be resolved in these experiments. Still, it was possible to fit the dissociation data to bi-exponential equations and to derive multiple dissociation rate constants, but in most experiments the fit was not statistically significantly better than a mono-exponential fit of the data. The presence of biphasic kinetics seems to be an observation common to other studies which have examined the kinetics of  $(R,S)$ - $[^3H]$ AMPA binding (Honoré and Drejer, 1988; Sawutz et al., 1995).

The calculated single-site  $k_{off}$  rates were identical for GluR1<sub>o</sub> and GluR3<sub>o</sub>, giving a  $t_{1/2}$  value of about 3.5 min for ligand dissociation; however, the single-site  $k_{on}$  rates were approximately five-fold different between GluR1<sub>o</sub> and GluR3<sub>o</sub>. Calculation from the kinetic data of the radioligand  $K_d$  at GluR1<sub>o</sub> and GluR3<sub>o</sub> was in reasonable agreement to the  $K_d$  values determined from equilibrium saturation binding experiments, with the kinetic  $K_d$  value for GluR3<sub>o</sub> showing about three-fold higher affinity than the saturation-derived  $K_d$  while the  $K_d$  for GluR1<sub>o</sub> was the same from either method. Attempts by others to compare the kinetically-derived  $K_d$  to the equilibrium-derived  $K_d$  have also found  $K_d$  values of somewhat higher affinity when calculated from the kinetic rate constants (Honoré and Drejer, 1988; Sawutz et al., 1995). Due to the absence of reliable estimates of the second  $k_{off}$  rate constant, it was not possible to isolate the corresponding second  $k_{on}$  rate constants, but nevertheless two  $k_{app}$  association rate constants could be measured, indicating multiple association rate constants. Again, the technical limitations of the filtration assay could be partly responsible for this difficulty in accurately resolving the  $k_{on}$  rate constants.

The disparity between the equilibrium binding experiments and the kinetic experiments, with regard to the number of binding sites, could be explained if co-operativity exists between two identical binding sites such that binding of the first agonist molecule influences to a similar extent the  $k_{on}$  and  $k_{off}$  rates of the second site. In this circumstance, the affinity of the second site for agonist would not be changed. Recently, it has been proposed from functional studies using GluR1 point mutants (Mano

and Teichberg, 1998) and from studies on outside-out patches from cultured hippocampal neurons (Clements et al., 1998) that the AMPA channel has a tetrameric structure consisting of two distinct agonist binding sites, where two molecules of agonist can activate the receptor fully. It is noteworthy that the NMDA receptor channel is also now thought to be tetrameric, where two molecules of agonist (glutamate) and two molecules of co-agonist (glycine) bind to the channel complex (Laube et al., 1998). Moreover, a three state allosteric model has been proposed (Paas, 1998) for the ionotropic glutamate receptors, where the channels exist in an equilibrium of resting (R), active (A) and desensitised (D) states. In this model, the channel consists of a tetrameric complex, where each subunit contains a binding site which can undergo transitions between open-lobe and closed-lobe conformations which give rise to the various channel states. Interestingly, one possible model of the AMPA channel proposed from the analysis of the activation kinetics consists of two identical, co-operative agonist binding sites, where the affinity of the first binding step is two to three fold higher than that of the second step (Clements et al., 1998). Hence, functional evidence supports a co-operative effect on AMPA channel activation which could also suggest, but not necessitate, a co-operativity in the agonist association and/or dissociation kinetics. The presence of two binding sites with only a two–three fold difference in ligand affinity would be virtually impossible to distinguish individually by radioligand binding experiments. Similarly, two–three fold differences in  $k_{on}$  or  $k_{off}$  rate constants would be very difficult to measure experimentally.

Hill values of unity were found for all drugs at all three of the receptor complexes in competition experiments, which concurs with the saturation data indicating a single binding site for each receptor. Of course, this could also be interpreted as multiple identical, independent binding sites (e.g., one binding site in each subunit forming the tetrameric/pentameric channel) which would not be individually resolved by these equilibrium experiments. Hill values of unity dispute any co-operativity in binding, which differs from the conclusions of functional experiments on the activation of AMPA receptors where co-operativity is proposed. It may well be that under the assay conditions for binding experiments, particularly the 4°C temperature, such co-operative effects are weak or absent (Hall et al., 1993b).

The pharmacological profiles of the homomeric and heteromeric GluR1<sub>o</sub> and GluR3<sub>o</sub> receptor complexes were very similar in the rank order of drug affinities: Tri-F-AMPA  $\approx$  AMPA  $\approx$  ACPA  $>$  L-glutamate  $>$  NBQX, CNQX  $>$  kainate; the exception being the somewhat lower affinity of glutamate at homomeric GluR3<sub>o</sub> receptors. Overall, the compounds tested exhibited the rank order typical of native AMPA receptor pharmacology (Honoré et al., 1988). Statistically, there was no difference in the affinities of any of the AMPA analogues between homo-

meric GluR3<sub>o</sub> or the heteromeric GluR1<sub>o</sub> + GluR3<sub>o</sub> receptor, however their affinities were slightly lower ( $P < 0.05$ , *t*-test) at homomeric GluR1<sub>o</sub>. The AMPA analogues had slightly different affinities amongst themselves at GluR1<sub>o</sub>, however there was only an approximately 2-fold range in the  $K_i$  values. Competition experiments of (*R,S*)-[<sup>3</sup>H]AMPA binding to native rat brain receptors using AMPA, ACPA and Tri-F-AMPA as inhibitors gave values (AMPA,  $IC_{50} = 79$  nM; ACPA,  $IC_{50} = 20$  nM; Tri-F-AMPA = 80 nM) that are in reasonable agreement with our data (Madsen and Wong, 1992; Madsen et al., 1992). Yet, in contrast to other reports (Madsen and Wong, 1992; Banke et al., 1997), we did not find ACPA to have the highest potency at these recombinant receptors but either a similar or lower affinity as AMPA and Tri-F-AMPA. Interestingly, the affinities of the AMPA analogues at the heteromeric complex were the same as at homomeric GluR3<sub>o</sub>, suggesting that for these agonists GluR3<sub>o</sub> is dominant in the heteromeric channel. On the other hand, for the endogenous agonist L-glutamate, GluR1<sub>o</sub> was dominant in the heteromeric complex. These patterns of agonist potency at the heteromeric complex were also seen for the  $EC_{50}$  data in our previous study (Banke et al., 1997), except for the compound ACPA where the  $EC_{50}$  was intermediate between homomeric GluR1<sub>o</sub> and homomeric GluR3<sub>o</sub>. Kainate was equipotent at the homomeric and heteromeric channels in terms of its  $EC_{50}$  but in terms of binding affinity, it had lowest affinity at GluR3<sub>o</sub>, highest at GluR1<sub>o</sub> and an intermediate affinity at the heteromeric complex. Hill values of unity argue against a mixed population of homomeric receptors and heteromeric receptors in the GluR1<sub>o</sub> + GluR3<sub>o</sub> infected Sf9 cell membranes. A significant population of either homomeric GluR1<sub>o</sub> or homomeric GluR3<sub>o</sub> would be expected to increase the Hill values significantly above unity for some compounds, especially for kainate which had the largest difference in affinity between the subunits. Although the affinity of kainate at the heteromeric complex was intermediate between the separate homomeric complexes, a Hill value of 0.98 was seen for kainate binding to the heteromeric complex, supporting the conclusion that the majority of the receptor population present must be in an heteromeric configuration. Of course, there could also be a small population of homomeric complexes, but then these should not be expected to contribute much to the overall  $K_i$  values determined for the heteromeric complex.

The mixed pattern of agonist affinity observed at the heteromeric complex, where either GluR1<sub>o</sub> or GluR3<sub>o</sub> can be dominant depending upon the agonist, is similar to what was seen in previous functional studies (Banke et al., 1997). The binding affinity of a given compound at the heteromeric complex mirrored that of the homomeric subunit for which it has highest affinity. The fact that kainate has an intermediate affinity at the heteromeric complex could indicate that the mode of binding of kainate is different from that of either AMPA or glutamate. Like-

wise, the fact that kainate is a less-desensitising agonist than AMPA or glutamate and that it yielded Hill coefficients of  $\approx 2$  in functional studies (Banke et al., 1997) had previously hinted at a difference in the way these agonists interact with AMPA receptors. The agonist ACPA had shown an 11-fold selectivity for GluR3<sub>o</sub> vs. GluR1<sub>o</sub> by its functional  $EC_{50}$  but here only exhibited a three-fold higher affinity for GluR3<sub>o</sub> (and for the heteromeric complex) compared to GluR1<sub>o</sub>. Now, if kainate is considered to be a non-desensitising agonist at the AMPA receptors, then comparing the relative maximal responses of kainate to ACPA (Banke et al., 1997; Fig. 2) it can be seen that ACPA is approximately 8-fold more desensitising at GluR3<sub>o</sub> than GluR1<sub>o</sub>, whereas AMPA itself is only about 4.5-fold more desensitising. This difference in the ability to induce desensitisation could imply that the efficacy of ACPA may therefore be higher at GluR3<sub>o</sub> than GluR1<sub>o</sub> and current experiments are underway to directly test this. This information should be useful in the design of yet even higher efficacy AMPA analogues and it may thus be possible to achieve subunit-selectivity in vivo by exploiting such differences in drug efficacy.

## Acknowledgements

ACPA, AMPA and Tri-F-AMPA were generously provided by Dr. Ulf Madsen, Department of Medicinal Chemistry, The Royal Danish School of Pharmacy. D.S.P. has been supported by the Alfred Benzon Foundation. This work was funded by grants from the Novo Nordisk Foundation, The Lundbeck Foundation and the Danish Medical Research Council (9700761).

## References

- Andersen, P.H., Tygesen, C.K., Rasmussen, J.S., Sørensen-Nielsen, L., Hansen, A., Hansen, K., Kierner, A., Stidsen, C.E., 1996. Stable expression of homomeric AMPA-selective glutamate receptors in BHK cells. *Eur. J. Pharmacol.* 311, 95–100.
- Arai, A., Silberg, J., Kessler, M., Lynch, G., 1995. Effect of thiocyanate on AMPA receptor mediated responses in excised patches and hippocampal slices. *Neuroscience* 66, 815–827.
- Banke, T.G., Schousboe, A., Pickering, D.S., 1997. Comparison of the agonist binding site of homomeric, heteromeric and chimeric GluR1<sub>o</sub> and GluR3<sub>o</sub> AMPA receptors. *J. Neurosci. Res.* 49, 176–185.
- Barnard, E.A., 1997. Ionotropic glutamate receptors: new types and new concepts. *Trends Pharmacol. Sci.* 18, 141–148.
- Beal, M.F., 1992. Mechanisms of excitotoxicity in neurologic diseases. *FASEB J.* 6, 3338–3344.
- Blackstone, C.D., Moss, S.J., Martin, L.J., Levey, A.I., Price, D.L., Huganir, R.L., 1992. Biochemical characterization and localization of a non-*N*-methyl-D-aspartate glutamate receptor in rat brain. *J. Neurochem.* 58, 1118–1126.
- Boulter, J., Hollmann, M., O'Shea-Greenfield, A., Hartley, M., Deneris, E., Maron, C., Heinemann, S., 1990. Molecular cloning and functional expression of glutamate receptor subunit genes. *Science* 249, 1033–1037.

- Choi, D.W., 1988. Glutamate neurotoxicity and diseases of the nervous system. *Neuron* 1, 623–634.
- Clements, J.D., Feltz, A., Sahara, Y., Westbrook, G.L., 1998. Activation kinetics of AMPA receptor channels reveal the number of functional agonist binding sites. *J. Neurosci.* 18, 119–127.
- Ferrier-Montiel, A.V., Montal, M., 1996. Pentameric subunit stoichiometry of a neuronal glutamate receptor. *Proc. Natl. Acad. Sci. USA* 93, 2741–2744.
- Giberti, A., Ratti, E., Gaviraghi, G., van Amsterdam, F.Th.M., 1991. Binding of DL-[<sup>3</sup>H]-α-amino-3-hydroxy-5-methylisoxazole-4-propionic acid (AMPA) to rat cortex membranes reveals two sites or affinity states. *J. Recept. Res.* 11, 727–741.
- Hall, R.A., Kessler, M., Lynch, G., 1992. Evidence that high- and low-affinity DL-α-amino-3-hydroxy-5-methylisoxazole-4-propionic acid (AMPA) binding sites reflect membrane-dependent states of a single receptor. *J. Neurochem.* 59, 1997–2004.
- Hall, R.A., Massicotte, G., Kessler, M., Baudry, M., Lynch, G., 1993a. Thiocyanate equally increases affinity for two DL-α-amino-3-hydroxy-5-methylisoxazolepropionic acid (AMPA) receptor states. *Mol. Pharmacol.* 43, 459–464.
- Hall, R.A., Kessler, M., Quan, A., Ambros-Ingerson, J., Lynch, G., 1993b. Cyclothiazide decreases [<sup>3</sup>H]AMPA binding to rat brain membranes: evidence that AMPA receptor desensitization increases agonist affinity. *Brain Res.* 628, 345–348.
- Hall, R.A., Hansen, A., Andersen, P.H., Soderling, T.R., 1997. Surface expression of the AMPA receptor subunits GluR1, GluR2 and GluR4 in stably transfected baby hamster kidney cells. *J. Neurochem.* 68, 625–630.
- Hattori, S., Okuda, K., Hamajima, K., Sakimura, K., Mishina, M., Kawamoto, S., 1994. Expression and characterization of the α2 subunit of the α-amino-3-hydroxy-5-methyl-4-isoxazole propionate (AMPA)-selective glutamate receptor channel in a baculovirus system. *Brain Res.* 666, 43–52.
- Hennegriff, M., Arai, A., Kessler, M., Vanderklish, P., Mutneja, M.S., Rogers, G., Neve, R.L., Lynch, G., 1997. Stable expression of recombinant AMPA receptor subunits: binding affinities and effects of allosteric modulators. *J. Neurochem.* 68, 2424–2434.
- Hollmann, M., Heinemann, S., 1994. Cloned glutamate receptors. *Annu. Rev. Neurosci.* 17, 31–108.
- Honoré, T., Drejer, J., 1988. Chaotropic ions affect the conformation of quisqualate receptors in rat cortical membranes. *J. Neurochem.* 51, 457–461.
- Honoré, T., Lauridsen, J., Krogsgaard-Larsen, P., 1982. The binding of [<sup>3</sup>H]AMPA, a structural analogue of glutamic acid, to rat brain membranes. *J. Neurochem.* 38, 173–178.
- Honoré, T., Davies, S.N., Drejer, J., Fletcher, E.J., Jacobsen, P., Lodge, D., Nielsen, F.E., 1988. Quinoxalinediones: potent competitive non-NMDA glutamate receptor antagonists. *Science* 241, 701–703.
- Hulme, E.C., Birdsall, N.J.M., 1992. Strategy and tactics in receptor-binding studies. In: Hulme, E.C. (Ed.), *Receptor–Ligand Interactions. A Practical Approach*, Oxford Univ. Press, Oxford, pp. 63–176.
- Hume, R.I., Dingleline, R., Heinemann, S.F., 1991. Identification of a site in glutamate receptor subunits that controls calcium permeability. *Science* 253, 1028–1031.
- Hunter, C., Wenthold, R.J., 1992. Solubilization and purification of an α-amino-3-hydroxy-5-methylisoxazole-4-propionic acid binding protein from bovine brain. *J. Neurochem.* 58, 1379–1385.
- Hunter, C., Wheaton, K.D., Wenthold, R.J., 1990. Solubilization and partial purification of α-amino-3-hydroxy-5-methyl-4-isoxazolepropionic acid binding sites from rat brain. *J. Neurochem.* 54, 118–125.
- Kawamoto, S., Onishi, H., Hattori, S., Miyagi, Y., Amaya, Y., Mishina, M., Okuda, K., 1991. Functional expression of the α1 subunit of the AMPA-selective glutamate receptor channel, using a baculovirus system. *Biochem. Biophys. Res. Commun.* 181, 756–763.
- Kawamoto, S., Hattori, S., Oiji, I., Hamajima, K., Mishina, M., Okuda, K., 1994. Ligand-binding properties and *N*-glycosylation of α1 subunit of the α-amino-3-hydroxy-5-methyl-4-isoxazole-propionate (AMPA)-selective glutamate receptor channel expressed in a baculovirus system. *Eur. J. Biochem.* 223, 665–673.
- Kawamoto, S., Hattori, S., Sakimura, K., Mishina, M., Okuda, K., 1995. *N*-linked glycosylation of the α-amino-3-hydroxy-5-methylisoxazole-4-propionate (AMPA)-selective glutamate receptor channel α2 subunit is essential for the acquisition of ligand-binding activity. *J. Neurochem.* 64, 1258–1566.
- Keinänen, K., Wisden, W., Sommer, B., Werner, P., Herb, A., Verdoorn, T.A., Sakmann, B., Seeburg, P.H., 1990. A family of AMPA-selective glutamate receptors. *Science* 249, 556–560.
- Keinänen, K., Köhr, G., Seeburg, P.H., Laukkanen, M.-L., Oker Blom, C., 1994. High-level expression of functional glutamate receptor channels in insect cells. *Biotechnology* 12, 802–806.
- Krogsgaard-Larsen, P., Brehm, L., Johansen, J.S., Vinzents, P., Lauridsen, J., Curtis, D.R., 1985. Synthesis and structure–activity studies on excitatory amino acids structurally related to ibotenic acid. *J. Med. Chem.* 28, 673–679.
- Kuusinen, A., Arvola, M., Oker Blom, C., Keinänen, K., 1995. Purification of recombinant GluR-D glutamate receptor produced in Sf21 insect cells. *Eur. J. Biochem.* 233, 720–726.
- Laemmli, U.K., 1970. Cleavage of structural proteins during the assembly of the head of bacteriophage T4. *Nature* 227, 680–685.
- Laube, B., Kuhse, J., Betz, H., 1998. Evidence for a tetrameric structure of recombinant NMDA receptors. *J. Neurosci.* 18, 2954–2961.
- Madsen, U., Wong, E.H.F., 1992. Heterocyclic excitatory amino acids. Synthesis and biological activity of novel analogues of AMPA. *J. Med. Chem.* 35, 107–111.
- Madsen, U., Ebert, B., Krogsgaard-Larsen, P., Wong, E.H.F., 1992. Synthesis and pharmacology of (*RS*)-2-amino-3-(hydroxy-5-trifluoromethyl-4-isoxazolyl)propionic acid, a potent AMPA receptor agonist. *Eur. J. Med. Chem.* 27, 479–484.
- Mano, I., Teichberg, V.I., 1998. A tetrameric subunit stoichiometry for a glutamate receptor–channel complex. *NeuroReport* 9, 327–331.
- Murphy, D.E., Snowhill, E.W., Williams, M., 1987. Characterization of quisqualate recognition sites in rat brain tissue using DL-[<sup>3</sup>H]-α-amino-3-hydroxy-5-methylisoxazole-4-propionic acid (AMPA) and a filtration assay. *Neurochem. Res.* 12, 775–782.
- Nayeem, N., Green, T.P., Martin, I.L., Barnard, E.A., 1994. Quaternary structure of the native GABA<sub>A</sub> receptor determined by electron microscopic image analysis. *J. Neurochem.* 62, 815–818.
- Nielsen, E.O., Cha, J.H., Honoré, T., Penney, J.B., Young, A.B., 1988. Thiocyanate stabilizes AMPA binding to the quisqualate receptor. *Eur. J. Pharmacol.* 157, 197–203.
- Olsen, R.W., Szamraj, O., Houser, C.R., 1987. [<sup>3</sup>H]AMPA binding to glutamate receptor subpopulations in rat brain. *Brain Res.* 402, 243–254.
- Paas, Y., 1998. The macro- and microarchitectures of the ligand-binding domain of glutamate receptors. *Trends Neurosci.* 21, 117–125.
- Sawutz, D.G., Krafte, D.S., Oleynek, J.J., Ault, B., 1995. AMPA (α-amino-3-hydroxy-5-methylisoxazole-4-propionic acid) receptors in human brain tissues. *J. Recept. Signal Transduction Res.* 15, 829–846.
- Sommer, B., Seeburg, P.H., 1992. Glutamate receptor channels: novel properties and new clones. *Trends Pharmacol. Sci.* 13, 291–296.
- Sommer, B., Keinänen, K., Verdoorn, T.A., Wisden, W., Burnashev, N., Herb, A., Köhler, M., Takagi, T., Sakmann, B., Seeburg, P.H., 1990. Flip and flop: a cell-specific functional switch in glutamate operated channels of the CNS. *Science* 249, 1580–1585.
- Sommer, B., Köhler, M., Sprengel, R., Seeburg, P.H., 1991. RNA editing in brain controls a determinant of ion flow in glutamate-gated channels. *Cell* 67, 11–19.
- Tarentino, A.L., Gómez, C.M., Plummer, T.H. Jr., 1985. Deglycosylation of asparagine-linked glycans by peptide: *N*-glycosidase F. *Biochemistry* 24, 4665–4671.
- Unwin, N., 1993. Neurotransmitter action: opening of ligand-gated ion channels. *Cell* 72, 31–41.
- Verdoorn, T.A., Burnashev, N., Monyer, H., Seeburg, P.H., Sakmann, B.,

1991. Structural determinants of ion flow through recombinant glutamate receptor channels. *Science* 252, 1715–1718.
- Vodyanoy, V., Bahr, B.A., Suppiramaniam, V., Hall, R.A., Baudry, M., Lynch, G., 1993. Single channel recordings of reconstituted AMPA receptors reveal low and high conductance states. *Neurosci. Lett.* 150, 80–84.
- Wentholt, R.J., Yokotani, N., Doi, K., Wada, K., 1992. Immunochemical characterization of the non-NMDA glutamate receptor using subunit-specific antibodies. *J. Biol. Chem.* 267, 501–507.
- Whetsell, W.O. Jr., 1996. Current concepts of excitotoxicity. *J. Neuropathol. Exp. Neurol.* 55, 1–13.
- Wu, T.-Y., Chang, Y.C., 1994. Hydrodynamic and pharmacological characterization of putative alpha-amino-3-hydroxy-5-methyl-4-isoxazolepropionic acid/kainate-sensitive L-glutamate receptors solubilized from pig brain. *Biochem. J.* 300, 365–371.